Histidine Decarboxylase Deficiency Causes Tourette Syndrome: Parallel Findings in Humans and Mice

Lissandra Castellan Baldan,[1] Kyle A. Williams,[1,2,16] Jean-Dominique Gallezot,[3,16] Vladimir Pogorelov,[1,16] Maximiliano Rapanelli,[1] Michael Crowley,[2] George M. Anderson,[2,4] Erin Loring,[2,5,8] Roxanne Gorczyca,[10] Eileen Billingslea,[1] Suzanne Wasylink,[1] Kaitlyn E. Panza,[2] A. Gulhan Ercan-Sencicek,[2,5] Kuakarun Krusong,[1,11] Bennett L. Leventhal,[12,13] Hiroshi Ohtsu,[14] Michael H. Bloch,[1,2] Zoë A. Hughes,[10] John H. Krystal,[1] Linda Mayes,[1,2,6,7] Ivan de Araujo,[1,15] Yu-Shin Ding,[3,17] Matthew W. State,[1,2,5,8,18] and Christopher Pittenger[1,2,7,9,*]
[1]Department of Psychiatry
[2]Child Study Center
[3]Department of Diagnostic Radiology
[4]Department of Laboratory Medicine
[5]Department of Genetics
[6]Department of Pediatrics
[7]Department of Psychology
[8]Program on Neurogenetics, Department of Genetics
[9]Integrated Neuroscience Research Program
Yale University School of Medicine, New Haven, CT 06520, USA
[10]Neuroscience Research Unit, Pfizer, Inc., Cambridge, MA 02139, USA
[11]Department of Biochemistry, Faculty of Science, Chulalongkorn University, Bangkok 10330, Thailand
[12]Nathan S. Kline Institute for Psychiatric Research, Orangeburg, NY 10962, USA
[13]Department of Child and Adolescent Psychiatry, New York University/NYU Langone Medical Center, New York, NY 10016, USA
[14]Graduate School of Engineering, Tohoku University, Sendai 980-8577, Japan
[15]John B. Pierce Laboratory, New Haven, CT 06519, USA
[16]These authors contributed equally to this work
[17]Present address: Department of Radiology, New York University, New York, NY 10016, USA
[18]Present address: Department of Psychiatry, University of California, San Francisco, San Francisco, CA 94143, USA
*Correspondence: christopher.pittenger@yale.edu
http://dx.doi.org/10.1016/j.neuron.2013.10.052

SUMMARY

Tourette syndrome (TS) is characterized by tics, sensorimotor gating deficiencies, and abnormalities of cortico-basal ganglia circuits. A mutation in histidine decarboxylase (Hdc), the key enzyme for the biosynthesis of histamine (HA), has been implicated as a rare genetic cause. Hdc knockout mice exhibited potentiated tic-like stereotypies, recapitulating core phenomenology of TS; these were mitigated by the dopamine (DA) D2 antagonist haloperidol, a proven pharmacotherapy, and by HA infusion into the brain. Prepulse inhibition was impaired in both mice and humans carrying Hdc mutations. HA infusion reduced striatal DA levels; in Hdc knockout mice, striatal DA was increased and the DA-regulated immediate early gene Fos was upregulated. DA D2/D3 receptor binding was altered both in mice and in humans carrying the Hdc mutation. These data confirm histidine decarboxylase deficiency as a rare cause of TS and identify HA-DA interactions in the basal ganglia as an important locus of pathology.

INTRODUCTION

Tourette syndrome (TS) is characterized by pathognomic motor and vocal tics, as well as by sensory and cognitive symptoms. It affects 0.3%–1.0% of the population. The onset of tics is typically in childhood; many patients, although not all, experience improvement of their symptoms in late adolescence or early adulthood.

Convergent evidence implicates dysregulation of cortico-basal ganglia circuits in TS (Albin, 2006; Leckman et al., 2010; Williams et al., 2013). Focal ischemic damage to the striatum, the input nucleus of the basal ganglia, can produce tics (Kwak and Jankovic, 2002), as can local striatal disinhibition in monkeys (McCairn et al., 2009). Disruption of dopaminergic modulation of this circuitry, in particular, is implicated, although the specific nature and etiology of this abnormality are unclear (Albin, 2006; Jankovic and Kurlan, 2011). Positron emission tomography (PET) imaging suggests increased striatal intrasynaptic dopamine (DA) in individuals with TS (Singer et al., 2002; Wong et al., 2008). The D2 DA receptor antagonists haloperidol and pimozide are the most efficacious pharmacological therapy for severe tics (Bloch, 2008; Du et al., 2010; Kurlan, 2010). Psychostimulant drugs such as D-amphetamine can trigger or worsen tics in patients (Leckman et al., 2010) and produce tic-like motor stereotypies in animals (Kelley, 2001).

The basal ganglia circuitry can be described, to a first approximation, as parallel cortico-striato-thalamo-cortical loops specialized for processing different types of behaviorally relevant information (Alexander et al., 1986; Choi et al., 2012; Haber and Knutson, 2010). Striatonigral neurons expressing the D1 DA receptor provide excitatory feedback to the cortex; striatopallidal neurons expressing the D2 DA receptor provide inhibitory feedback. Dynamic balance between these parallel pathways contributes to regulating diverse behaviors (Albin et al., 1989; Graybiel, 2008; Grillner et al., 2013; Haber and Knutson, 2010).

TS has a heritability of approximately 0.58 (Davis et al., 2013). Causative mutations and major risk alleles have proven elusive (Bloch et al., 2011; O'Rourke et al., 2009; State, 2011). A recent genome-wide association study failed to identify any common polymorphisms with genome-wide statistical significance (Scharf et al., 2013). In this setting, rare, highly penetrant mutations are of particular value in the generation and testing of pathophysiological hypotheses.

A recent study of a two-generation pedigree in a family with a high incidence of TS identified a rare segregating nonsense mutation, *Hdc* W317X, in the *l-histidine decarboxylase* (*Hdc*) gene (Ercan-Sencicek et al., 2010). Histidine decarboxylase (HDC) is required for the generation of histamine (HA) from histidine (Haas et al., 2008). Subsequent analyses have also implicated disruption of *Hdc* (Karagiannidis et al., 2013) or of histaminergic signaling more generally (Fernandez et al., 2012) in TS. However, the causal connection between reduced HDC activity and TS symptoms and the pathophysiological links between *Hdc* disruption and TS-relevant neurobiological abnormalities remain unclear.

HA is produced by neurons in the tuberomamillary nucleus of the posterior hypothalamus that project throughout the central nervous system (CNS) (Haas et al., 2008). Pharmacological studies show that enhancing central HA production modulates stereotypy produced by methamphetamine (Joshi et al., 1981; Kitanaka et al., 2007) or apomorphine (Paul et al., 2000).

The *Hdc* W317X mutation is rare; it has not been identified outside of the index family (Ercan-Sencicek et al., 2010). However, it has several characteristics that make it optimal for testing in an animal model. It is dominantly acting and of high penetrance. The enzymatic activity of HDC is well understood (Haas et al., 2008), and the nonsense mutation completely abrogates biosynthetic capacity (Ercan-Sencicek et al., 2010). Finally, the hypothesized ability of HA to modulate DA levels in the CNS (Haas et al., 2008) leads to a testable hypothesis: that reduced HA production produces TS phenomenology through dysregulation of dopaminergic modulation of the basal ganglia.

RESULTS

Individuals Carrying a Hypomorphic *Hdc* Allele Exhibit Tics; *Hdc* Knockout Mice and Heterozygotes Exhibit Potentiated Tic-like Stereotypies

The clinical histories of the carriers of the *Hdc*W317X mutation have been described elsewhere (Ercan-Sencicek et al., 2010). Diagnoses were confirmed using the Structured Clinical Interview for *DSM-IV* (First et al., 1997) (Table S1 available online). Tics were within a typical range of severity. There was no significant correlation between age and tic severity, as measured by the Yale Global Tic Severity Scale (Leckman et al., 1989; $p > 0.4$). Four of the nine had comorbid obsessive-compulsive disorder (OCD) symptoms; three had a history of depressive symptoms; and one had high-functioning autism. None were treated with high-potency D2 antagonists such as haloperidol (Bloch, 2008). Three were on SSRI antidepressants for treatment of comorbid depressive, anxiety, and OCD symptoms.

We turned to a mouse model to establish the causal relationship of *Hdc* disruption to key behavioral and neurochemical characteristics of TS. *Hdc* W317X produces a truncated protein without enzymatic activity (Ercan-Sencicek et al., 2010; see Figure 1A). *Hdc* knockout (KO) mice produce no HDC protein (Krusong et al., 2011; Ohtsu et al., 2001). [HA] was reduced in +/− mice, confirming haploinsufficiency, and was undetectable in −/− animals (Figure 1B).

Psychostimulants can potentiate tics and tic-like stereotypies. We assessed motor stereotypies before and after administration of a single intraperitoneal (i.p.) dose of D-amphetamine (8.5 mg/kg in sterile saline, the threshold for production of observable motor stereotypies in wild-type animals on this genetic background).

$Hdc^{+/−}$ and $Hdc^{−/−}$ mice showed normal baseline locomotion (Figure 1C), exploratory rearing, and center occupancy in an open field (Figure 1D) and no evident spontaneous motor stereotypies. Wild-type mice showed locomotor activation after amphetamine, which was attenuated in $Hdc^{+/−}$ and $Hdc^{−/−}$ mice (Figure 1C). Reduced locomotion is often seen in wild-type mice administered high doses of amphetamine, as stereotypical movements compete with it. We observationally quantified a range of stereotypies after D-amphetamine (Kelley, 2001); the majority consisted of repetitive focused sniffing and orofacial movements (see Movies S1, S2, and S3). KO mice showed markedly increased motor stereotypies (Figure 1E).

The reduced locomotion in heterozygotes suggests that they were engaged in stereotypies that competed with locomotor behavior but fell below the threshold of detection. We administered a higher dose of D-amphetamine (10 mg/kg) in an independent cohort of mice to see whether enhanced stereotypies would manifest in heterozygotes. Locomotor activation was again attenuated in +/− and −/− mice (Figure S1E). At this higher dose, many of the KOs became immobile, rendering quantification of stereotypy impossible. Heterozygotes now showed increased stereotypy (Figure 1F). Thus, *Hdc* deficiency potentiates tic-like stereotypies.

Stereotypies in *Hdc* KO Mice Are Mitigated by Haloperidol Pretreatment

We tested the responsiveness of tic-like stereotypies to haloperidol, a DA D2 receptor antagonist, in an independent cohort of *Hdc* mice (Figure 2A). HA levels go up during the active circadian phase (Haas et al., 2008; Figures 5B and S5B). Thus, behavioral phenotypes may vary across the light-dark cycle. We performed these experiments at night to replicate the core phenotype while HA levels are elevated in wild-type animals (because mice are nocturnal).
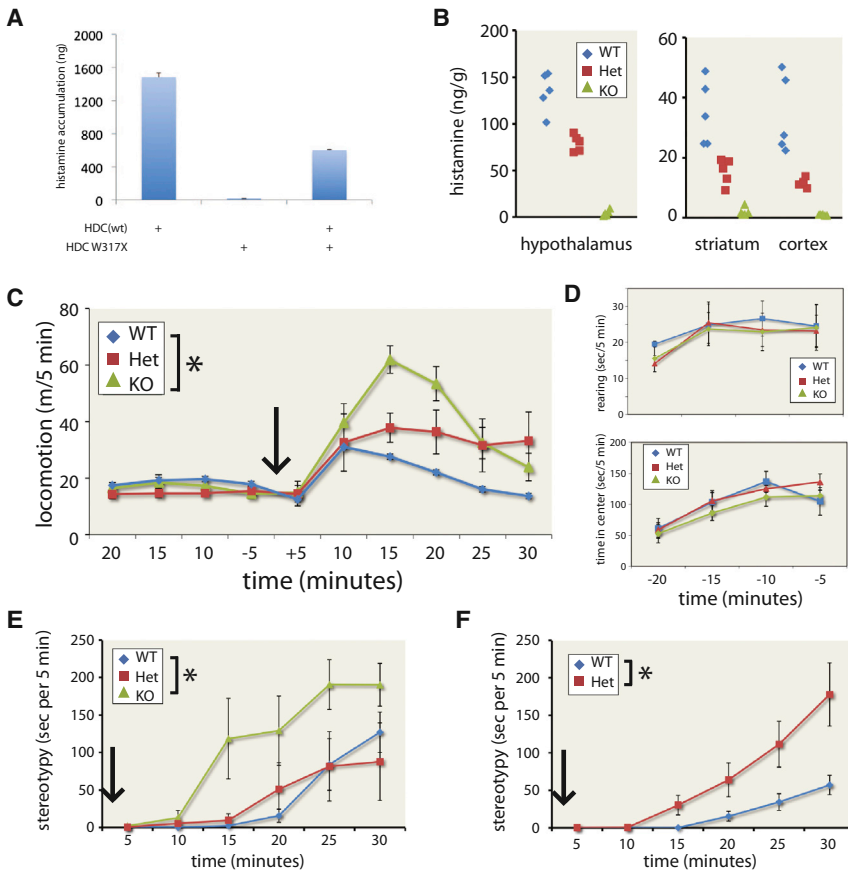
Figure 1. Reduced HA Levels and Stereotypy in *Hdc* KO and Haploinsufficient Mice

(A) *Hdc* W317X was devoid of enzymatic activity; addition of equimolar *Hdc* W317X to a constant amount of wild-type *Hdc* mRNA reduced HA accumulation, confirming the in vitro dominant-negative effect of this mutant.

(B) $Hdc^{+/-}$ and $Hdc^{-/-}$ mice showed reduced whole-tissue HA in hypothalamus (left), striatum, and neocortex (right), confirming efficacy of the KO and haploinsufficiency in +/− mice (n = 5 per genotype). WT, wild-type; Het, $Hdc^{+/-}$ (heterozygote).

(C) All genotypes showed similar exploratory activity over 20 min in a novel open field. Following 8.5 mg/kg D-amphetamine (i.p., in normal saline), WT mice showed locomotor activation, which was attenuated in −/− and +/− mice (RM-ANOVA, genotype, F[2,15] = 3.8, p = 0.04; Time × Genotype, F[10,75] = 2.15, p = 0.02; n = 6 per genotype).

(D) Prior to amphetamine, KO mice showed normal rearing (upper panel) and center occupancy time (lower panel) in the open field, confirming normal exploratory activity and anxiety.

(E) KO mice showed markedly increased stereotypy, beginning 10 min after D-amphetamine injection. RM-ANOVA, genotype: F[2,15] = 3.8; p = 0.04; Time × Genotype, F[10,75] = 1.83, p = 0.06.

(F) At a higher dose of D-amphetamine (10 mg/kg), several −/− mice became completely immobile, making quantification of stereotypy impossible; +/− mice, however, now showed enhanced stereotypy (RM-ANOVA, genotype: F[1,10] = 7.70, p = 0.01; Time × Genotype: F[5,50] = 4.36, p = 0.002; n = 6 per group). *p < 0.05.

Group data are represented as mean ± SEM. See also Figure S1.

Haloperidol pretreatment produced a modest but statistically significant reduction in locomotor activity after amphetamine that did not differ across genotypes (Figures 2B and S2). $Hdc^{-/-}$ mice pretreated with i.p. saline again exhibited tic-like stereotypies after 8.5 mg/kg D-amphetamine; heterozygotes also showed elevated stereotypies (Figure 2C). This experiment was conducted in older animals (7–9 months) than the initial characterization (Figures 1E and 1F; 3–7 months), suggesting that stereotypy does not vary with age; this recapitulates the persistence of tics seen in adult carriers of the *Hdc* W317X mutation (Table S1).

Pretreatment with 0.3 mg/kg haloperidol attenuated stereotypies in −/− mice and eliminated them in heterozygotes (Figures 2D and 2F). Pretreatment with 0.6 mg/kg haloperidol eliminated stereotypies in all genotypes (Figures 2E and 2F). The haloperidol effect was significant in the $Hdc^{-/-}$ mice, considered in isolation (repeated measures [RM]-ANOVA: Haloperidol Dose × Time interaction, F[10,40] = 2.19, p = 0.039) but not in the other genotypes. Collapsing across postamphetamine time points, there was a main effect of genotype in the saline-treated condition (Figure 2F; ANOVA of genotype and treatment order, F[2,10] = 5.70, p = 0.022) that was attenuated at the 0.3 mg/kg (F[2,9] = 2.09, p = 0.18) and 0.6 mg/kg doses of haloperidol (F[2,9] = 0.86, p > 0.4). All animals received the highest haloperidol dose on the third day; key effects remained significant when analysis was restricted to only saline and 0.3 mg/kg

haloperidol, with treatment order randomized and the investigator blind to treatment: RM-ANOVA with treatment order as an independent factor (main effect of haloperidol, F[1,55] = 6.99, p = 0.023; main effect of genotype, F[2,11] = 3.99, p = 0.05; main effect of time, F[5,55] = 6.46, p < 0.001; Time × Genotype interaction, F[10,55] = 2.69, p = 0.009).

To better quantify the potentiated stereotypies in $Hdc^{+/-}$ and $Hdc^{-/-}$ mice, we combined data from the three experiments described earlier (Figures 1E, 1F, and 2C). In the combined data set (n = 17 +/+, 17 +/−, and 11 −/− mice), the differential induction of stereotypies across genotypes was highly significant (RM-ANOVA with genotype and experiment as between-subjects factors: main effect of genotype, F[2,35] = 10.8, p < 0.001; main effect of time, F[5,175] = 26.8, p < 0.001; Time × Genotype interaction, F[10,175] = 3.6, p < 0.001). Bonferroni-corrected post hoc comparisons showed that −/− mice have more stereotypies than +/+ mice (p < 0.001) and +/− mice (p = 0.004); +/− mice had nominally more stereotypies than +/+ mice, but this difference did not reach significance.

Stereotypy in *Hdc* KO Mice Is Mitigated by HA Repletion

If the potentiation of tic-like stereotypies is a direct consequence of HA reduction, then it should be mitigated by direct repletion of brain HA. We infused HA or saline intracerebroventricularly (i.c.v.) immediately before administering amphetamine in $Hdc^{+/+}$ and $Hdc^{-/-}$ mice. Stereotypy was delayed and reduced
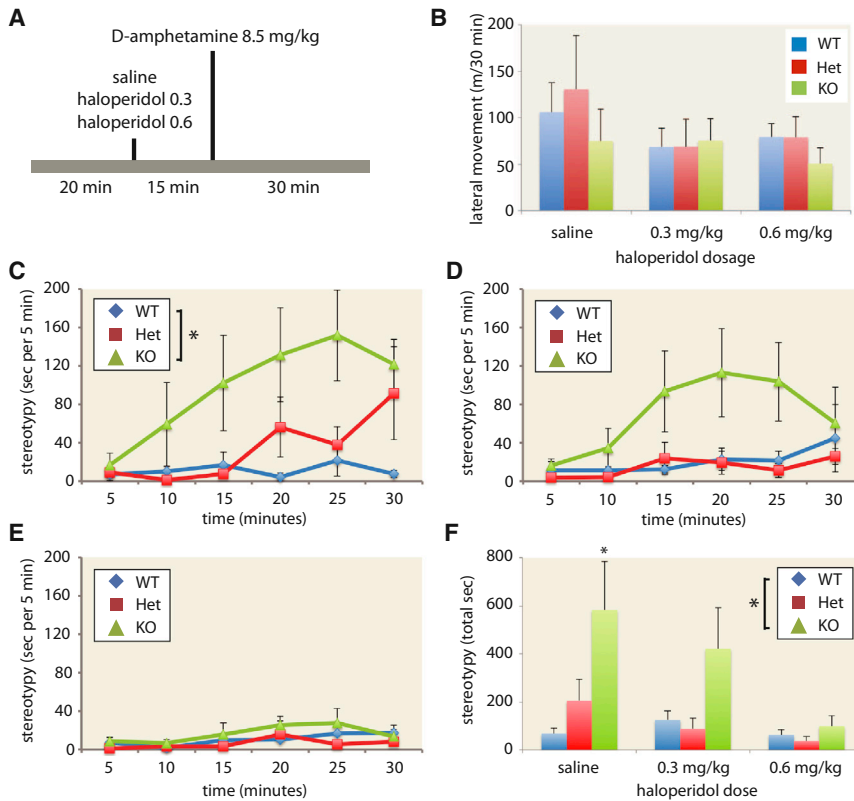
Figure 2. Attenuation of Tic-like Stereo-typies in $Hdc^{+/-}$ and $Hdc^{-/-}$ Mice after Pretreatment with Haloperidol

(A) Experimental design.

(B) Haloperidol pretreatment produced a modest reduction in amphetamine-induced locomotion (F [2,22] = 6.86, p = 0.005) that did not vary by genotype (main effect of genotype: F[2,11] = 0.27, p > 0.75; Genotype × Dose interaction: F[4,22] = 0.36, p > 0.8; n = 5 mice per group).

(C) Tic-like stereotypy was again seen in $Hdc^{+/-}$ and $Hdc^{-/-}$ mice after saline pretreatment (n = 5 mice per group; RM-ANOVA with genotype and treatment order as independent factors: main effect of genotype, F[2, 10] = 5.7, p = 0.022; main effect of time, F[5,50] = 5.7, p < 0.001; Genotype × Time interaction, F[10,50] = 2.4, p = 0.019).

(D) Pretreatment with 0.3 mg/kg haloperidol attenuated the development of stereotypies.

(E) Pretreatment with 0.6 mg/kg haloperidol elimi-nated stereotypies in all genotypes (RM-ANOVA across all haloperidol doses: main effect of time, F [5,45] = 6.67, p < 0.001; main effect of haloperidol dose, F[2,18] = 4.42, p = 0.027; main effect of genotype, F[2,9] = 4.4, p = 0.046; Genotype × Time, F[10,45] = 2.10, p = 0.044).

(F) Total stereotypies across the 30 min following amphetamine treatment are shown for each condition (RM-ANOVA: Main effect of genotype, F[2,9] = 4.39, p = 0.046; main effect of haloperidol treatment, F[2,18] = 4,42, p = 0.027). *p < 0.05 versus wild-type, main effect, or

Bonferroni-corrected post hoc analysis. n = 5 animals per genotype; see Experimental Procedures for detailed methods. Group data are represented as mean ± SEM. See also Figure S2.

in amplitude in surgically cannulated animals, necessitating a modified monitoring paradigm (see Experimental Procedures). All animals received both saline and HA pretreatment, in counter-balanced order.

When saline was given i.c.v. immediately before amphet-amine, we again observed focused sniffing stereotypies (Figures 1E, 1F, 2C, and 2F) in both +/+ and −/− animals. As in previous experiments, they were elevated in $Hdc^{-/-}$ animals (Figure 3A).

HA pretreatment almost completely eliminated these focused stereotypies, in both genotypes (Figures 3A and 3B). Because of a lack of variance in measured stereotypies in the HA-pretreated animals, analysis of HA effects was performed using nonpara-metric ANOVA-like statistics (see Experimental Procedures). There was a robust effect of HA pretreatment (df = 1, ANOVA-type statistic [ATS] = 28.47, p < 0.0001) and of time (df = 1, ATS = 8.03, p < 0.0001) and a HA × Time interaction (df = 2.8, ATS = 6.69, p = 0.0002). Collapsing across postamphetamine time points, stereotypies were dramatically reduced by HA pretreatment in both genotypes (Mann-Whitney U test: p < 0.05 for $Hdc^{+/+}$ mice, p < 0.001 for $Hdc^{-/-}$ mice).

Direct delivery of HA into the brain is sedating (Kalivas, 1982; Kamei et al., 1983; Onodera and Ogura, 1981). Consistent with this, HA-pretreated mice showed reduced locomotor activity, (Figure S3B), especially initially; HA-treated $Hdc^{-/-}$ mice showed greater locomotor activation in the second half of the hour than HA-treated $Hdc^{+/+}$ mice, permitting dissociation of

effects on locomotion and stereotypy. In the first 30 min following HA (Figure 3C, left panel) there was a significant effect of HA (ANOVA: F[1,38] = 25.9, p < 0.001) with a trend-level Genotype × HA interaction (F[1,25] = 2.96, p = 0.093) and post hoc differences between the HA-treated and saline-treated groups. In the latter 30 min, the effect of HA was at trend level (F[1,38] = 2.90, p = 0.097) and the Genotype × HA interaction was significant (F[1,38] = 5.2, p = 0.028), with only the HA-treated +/+ animals showing significantly reduced activity (Figure 3C). Since the reductions in stereotypy seen in HA-pretreated $Hdc^{-/-}$ mice are apparent during the latter half of the first hour following amphetamine administration (Figure 3A), this rules out the possibility that the reduction is due simply to sedation. Nonstereotypic, exploratory sniffing was not altered by HA pretreatment (see Figures S3C and S3D).

Excessive grooming has been proposed to be a behavioral manifestation of OCD-like pathology (Shmelkov et al., 2010; Welch et al., 2007). It is surprising that HA infusion increased grooming in both genotypes (Figures S3E and S3F). Stereotypies and abnormal grooming may reflect distinct perturbations of the basal ganglia circuitry.

Sensorimotor Gating Deficits in Humans and Mice Carrying a Mutant *Hdc* Gene

TS is characterized by deficits in sensorimotor gating, reflected in a deficit in prepulse inhibition (PPI) of startle (Castellanos
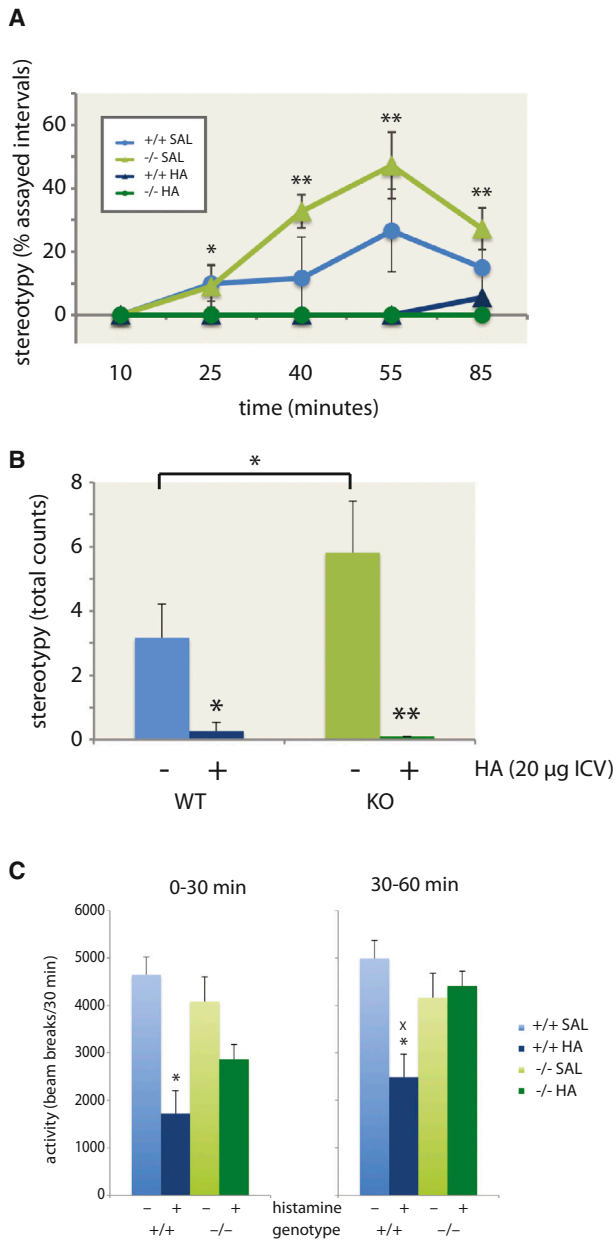
Figure 3. Mitigation of Stereotypies by HA Repletion

(A) Increased stereotypies were again seen after D-amphetamine, and were potentiated in $Hdc^{-/-}$ animals, after i.c.v. saline (SAL). These stereotypies were completely eliminated by HA infusion (20 μg). Saline groups: RM-ANOVA of genotype and treatment order, main effect of genotype, F[1,19] = 3.22, p = 0.09, significant at alpha = 0.1 for a predicted directional effect; main effect of time, F[4,76] = 9.26, p < 0.001; n = 12 mice of each genotype. See Results for analysis of HA effects. WT, wild-type.

(B) Stereotypies showed a similar temporal trajectory in $Hdc^{+/+}$ and $Hdc^{-/-}$ mice, peaking in the second half hour after amphetamine injection; they were absent throughout this time after HA infusion in both genotypes.

(C) HA infusion led to reduced locomotor activation following amphetamine; however, this effect dissociated from the mitigation of stereotypies, as locomotor activity recovered in the second 30 min following amphetamine injection in $Hdc^{-/-}$ animals. *p < 0.05; **p < 0.01; x indicates p < 0.05 genotype effect. Group data are represented as mean ± SEM. See also Figure S3.

et al., 1996; Swerdlow et al., 2001; Terrados et al., 2012). PPI can be measured in humans and experimental animals using nearly identical protocols (Baldan Ramsey et al., 2011; Swerdlow, 2012). PPI deficits are also seen in other neuropsychiatric conditions, including OCD (Ahmari et al., 2012; de Leeuw et al., 2010; Hoenig et al., 2005) and schizophrenia (Braff et al., 1978; Turetsky et al., 2007). However, in the context of a genetic abnormality independently associated with TS, an endophenotype such as a PPI deficit can provide valuable reinforcing face validity.

We tested PPI in patients carrying the *Hdc* W317X mutation. PPI of the startle response to an auditory stimulus, monitored by electromyogram of the orbicularis oculi muscle, was assessed in the nine individuals carrying the *Hdc* W317X mutation and in nine age- and sex-matched controls, using standard procedures (Lipschitz et al., 2005). TS patients had reduced auditory PPI, measured either 15 or 20 ms after the onset of the startle stimulus (Figure 4A; Figure S4A). There was no between-group difference in startle amplitude on trials in which no prepulse was presented (t[16] = 0.82; p = 0.43 at 20 ms). PPI within the TS group was variable (Figure S4A). There was a weak negative association between PPI and age among the patients that did not reach statistical significance (Figure 4B). Heterogeneity of PPI in the patient group was not explained by gender, medication status, comorbidity, or other clinical variables (Figures S4B–S4G). These data represent the first time, to our knowledge, that a PPI deficit has been associated with a specific genetic abnormality in humans (Kohl et al., 2013).

We predicted that *Hdc* KO mice would recapitulate this endophenotype. We tested auditory PPI in mice, following a standard protocol (Baldan Ramsey et al., 2011). $Hdc^{+/-}$ and $Hdc^{-/-}$ mice exhibited a significant PPI deficit (Figures 4C and S4H).

There was a trend toward higher baseline startle in +/− and −/− mice than in +/+ controls (Figure S4I), and PPI correlated negatively with baseline startle across all animals (Figure 4D). However, statistical significance was increased, not attenuated, when startle was included as a covariate, controlling for the possibility that a genotype effect on startle intensity underlies the PPI phenotype (Figures 4D and S4J). There was a nominal association of age with an increased PPI phenotype in the KO mice, although it did not approach statistical significance (Figure 4E). We repeated this experiment at night, with similar results (Figures 4F, S4O, and S4P). $Hdc^{-/-}$ mice have been reported to display increased anxiety (e.g., Dere et al., 2004), which may affect startle; however, we found no evidence of altered anxiety in the elevated plus maze or the open field in these animals, possibly because they are on a different genetic background than those described previously (Figures 1D and S1A–S1D).

Striatal DA Is Negatively Regulated by HA and Is Dysregulated in *Hdc* KO Mice

HA has been hypothesized to regulate DA negatively (Haas et al., 2008; Schlicker et al., 1994). To examine this in vivo, we infused HA i.c.v. into wild-type mice and measured striatal DA using microdialysis. HA i.c.v. (20 μg in sterile saline) led to a marked reduction in DA in the contralateral striatum (Figure 5A), accompanied by reduced activity (data not shown). In
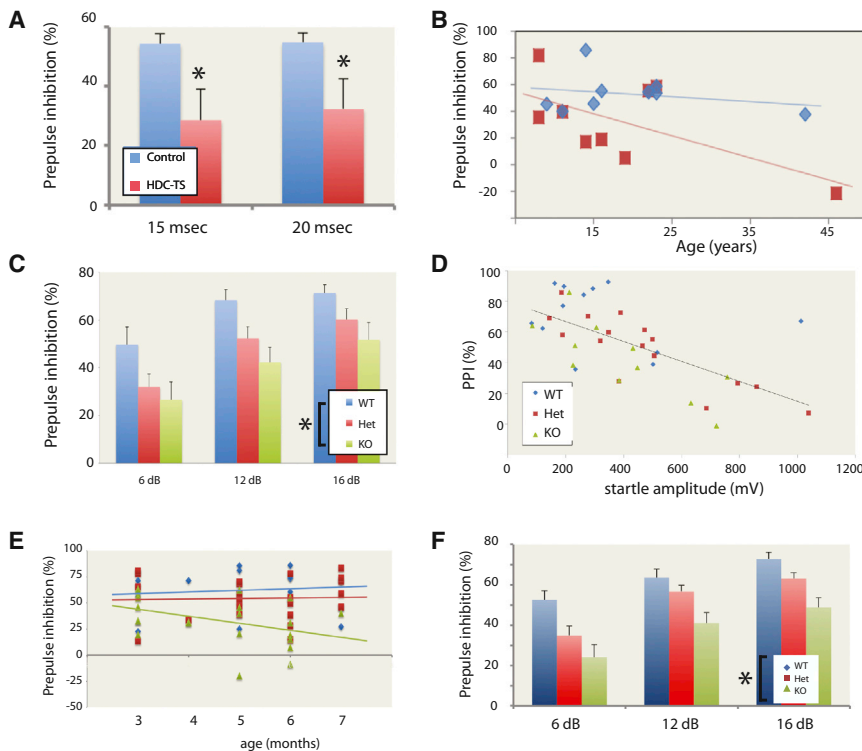
Figure 4. Impaired PPI in Humans and Mice with Deficient HDC Activity

(A) Patients carrying the *Hdc* W317X mutation showed impaired PPI, measured 15 and 20 ms after the startle stimulus. n = 9 *Hdc* W317X carriers and 9 matched controls. One-tailed heteroskedastic t test: 15 ms, t = 2.14, p = 0.02; 20 ms, t = 1.81, p = 0.04.

(B) There was a weak negative association between PPI and age among the patients, but it did not reach statistical significance (data are shown for the 20 ms time point, p = 0.08; p = 0.16 at 15 ms). The association of PPI with age did not approach significance in controls. The effect of genotype on PPI remained significant after covarying for age (20 ms: main effect of genotype, F [1,15] = 4.45, p = 0.05; 15 ms: main effect of genotype, F[1,15] = 5.89, p = 0.03).

(C) $Hdc^{+/-}$ and $Hdc^{-/-}$ mice showed a deficit in auditory PPI at three prepulse intensities. RM-ANOVA: F[2,31] = 4.50; p = 0.019; n = 12 +/+, 16 +/−, and 11 −/− mice. WT, wild-type; Het, $Hdc^{+/-}$ (heterozygote).

(D) $Hdc^{+/-}$ and $Hdc^{-/-}$ mice showed enhanced startle, but the PPI phenotype was not explained by this increased startle. r = −0.643; p < 0.001; data shown are for the first PPI block. A similar effect was seen in the second block: r = −0.622, p < 0.001. When analyzed separately, this correlation was seen in heterozygotes (n = 16; r = −0.842; p < 0.001) and KOs (n = 11; r = 0.780; p = 0.005) but not in WT mice (n = 12; r = −0.244; p > 0.4). RM-ANCOVA: F[2,35] = 6.67; p = 0.004; main effect of prepulse intensity: F[1,35] = 65.1, p < 0.001.

(E) In a larger group of mice tested at different ages, the PPI phenotype did not change with age. RM-ANCOVA: main effect of genotype, F[2,56] = 3.79, p = 0.03; age, F[1,56] = 0.12, p > 0.7; n = 16 +/+, 23 +/−, and 23 −/− mice.

(F) This PPI phenotype was replicated when animals were tested in their dark phase. RM-ANOVA across the three prepulse intensities: F[2,72] = 8.0, p = 0.001; n = 21 +/+, 26 +/−, and 28 −/− mice.

All data are represented as mean ± SEM. *p < 0.05. See also Figure S4.

contrast, saline infusion had no lasting effect on striatal HA levels.

Hdc KO mice have increased striatal DA turnover (Dere et al., 2003). We assayed striatal [HA] and [DA] using in vivo microdialysis (Figures S5A, S5B, and S5D). HA levels were dramatically reduced in −/− mice (Figure 5B). In +/+ animals, [HA] increased during the dark (active) phase (Figure S5E), reflecting its role in arousal (Haas et al., 2008).

There was not a main effect of genotype on unnormalized daytime striatal [DA] levels in KO mice, although given the variability inherent in unnormalized microdialysis data, we cannot rule out a subtle abnormality. However, there was a significant Genotype × Time interaction, with increased [DA] in $Hdc^{-/-}$ mice in the dark phase, when HA is high in +/+ mice (Figure 5C). We isolated this effect by normalizing DA to the daytime baseline, thereby reducing between-subjects technical variability (see Figures S5E and S5F); analysis of normalized data confirmed a significantly higher DA in $Hdc^{-/-}$ mice during the dark cycle (Figure 5D).
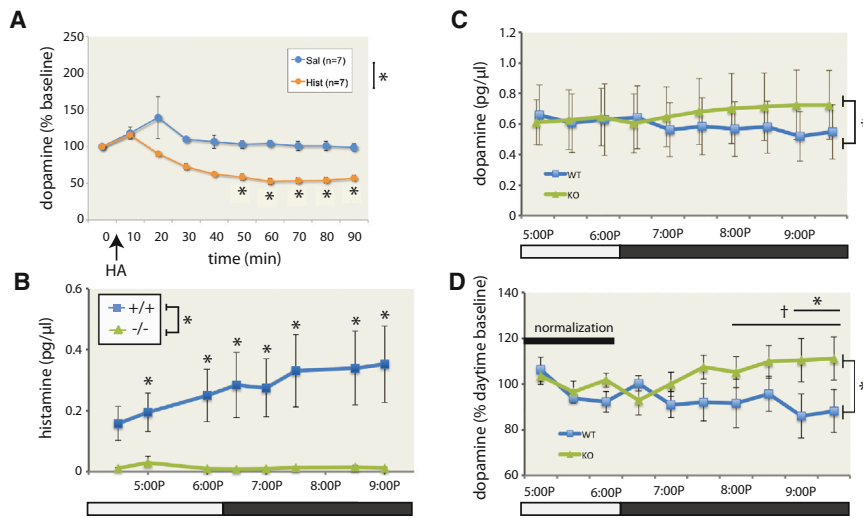
DA Signaling Is Enhanced and Striasomal Activation Is Potentiated in $Hdc^{-/-}$ Mice

We examined *Fos* immunoreactivity as a surrogate marker for neuronal activation in striatal medium spiny neurons (Figures

6A and 6B). *Fos* is upregulated in D1-expressing medium spiny neurons (MSNs) in response to pharmacological elevations in DA (Young et al., 1991). Doses of psychostimulants that produce stereotypy preferentially upregulate *Fos* in MSNs in striatal compartments known as striasomes (Canales and Graybiel, 2000); an imbalance between activation of striasomal and matrix MSNs may lead to stereotypies and tics (Canales and Graybiel, 2000; Crittenden and Graybiel, 2011).

At baseline, *Fos* was modestly elevated in both striasomes and matrix of $Hdc^{-/-}$ mice, relative to $Hdc^{+/+}$ sibling controls (Figure 6C). As this tissue was collected during the day, this suggests DA dysregulation in $Hdc^{-/-}$ mice even in the inactive phase. There was nominally higher *Fos* in the matrix than in the striasomes across genotypes, but this did not reach statistical significance (F[1,10] = 0.8, p = 0.4).

Forty-five minutes after amphetamine injection (5 mg/kg D-amphetamine, to avoid saturating the response) there was a marked increase in *Fos* expression in both genotypes and in both compartments. *Fos* was greatly increased in striasomes of $Hdc^{-/-}$ mice, relative both to matrix in the same animals and to striasomes in controls (Figure 6D). The genotype effect was restricted to the striasomal compartment; the striasome-matrix difference was thus markedly enhanced in $Hdc^{-/-}$ mice.

Figure 5. HA Regulates Striatal DA

(A) HA (20 µg) or saline was infused i.c.v. into wild-type mice, as in Figure 3. DA in microdialysate from the contralateral striatum was markedly reduced, starting 20 min after HA administration. ns = 7 HA and 7 saline; RM-ANOVA: main effect of time, $F[9,108] = 10.5$, $p < 0.001$; main effect of HA, $F[1,12] = 28.6$, $p < 0.001$; Time × HA, $F[9,108] = 3.9$, $p < 0.001$.

(B) HA in striatal microdialysate was dramatically reduced in $Hdc^{-/-}$ mice relative to controls. RM-ANOVA: main effect of genotype, $F[1,14] = 6.60$, $p = 0.02$; Genotype × Time, $F[7,98] = 4.23$, $p < 0.001$; n = 8 animals per group.

(C) DA in striatal microdialysate showed a significant Genotype × Time interaction: $F[9,126] = 2.70$, $p = 0.007$; n = 8 animals per group.

(D) Microdialysis data were normalized to the daytime baseline to reduce between-animal technical variability. The interaction was again apparent (main effect of genotype, $F[1,14] = 2.99$, $p = 0.11$; Genotype × Time, $F[9,126] = 2.85$, $p = 0.004$); the genotype difference reached trend level across the final four time points (RM-ANOVA, $F[1,14] = 3.8$, $p = 0.07$) and significance across the final two ($F[1,14] = 4.6$, $p = 0.05$). $^{†}p < 0.1$.

All data represented as mean ± SEM. *$p < 0.05$. See also Figure S5.

Dysregulated D2+D3 Receptors in the Basal Ganglia of TS Patients Carrying the *Hdc* W317X Mutation

DA cannot be directly assayed in vivo in humans. However, dysregulation of dopaminergic modulation within the basal ganglia may be reflected in compensatory changes in DA receptors. DA receptors can be examined in vivo in patients using PET.

We focused on D2 and D3 DA receptors, because D2 antagonists have therapeutic efficacy in TS (Bloch, 2008) and because these receptors exhibit homeostatic change upon chronic hyperstimulation. D3 receptors on midbrain dopaminergic neurons may function as inhibitory autoreceptors (Stanwood et al., 2000a; White and Wang, 1984); substantia nigra (SN) D2/D3 binding is increased after chronic stimulation in rats (Stanwood et al., 2000b) and in chronic users of cocaine (Payer et al., 2013). Striatal D2 receptors are downregulated after chronic pharmacological stimulation in rats and humans (Stanwood et al., 2000b; Volkow et al., 2009) and in hyperdopaminergic mice (Fauchey et al., 2000).

PET ligand binding permits limited discrimination between D2 and D3 receptors. We used ^{11}C-PHNO, an agonist tracer that binds to high-affinity D2 and D3 receptors, with preference for D3. This allows imaging of both the dorsal striatum, where D2 receptor density is very high, and the SN, where D3 receptors predominate (Graff-Guerrero et al., 2008; Narendran et al., 2006; Rabiner et al., 2009; Tziortzi et al., 2011).

PET scanning was performed in the four adult patients; usable data were acquired in three and compared to data from nine controls matched for age, sex, and body mass index (Figures 7A and 7B; Tables S2 and S3). Plasma free fraction and nonspecific PHNO binding did not differ between groups (Figures S6A–S6C). There was a significant increase in PHNO binding in patients in the globus pallidus (GP) and SN (Figure 7C). This difference did not survive correction for multiple comparisons in the GP ($t[10] = 2.29$; uncorrected $p = 0.045$) but did in the substantia nigra ($t[10] = 3.27$, uncorrected $p = 0.008$; see also Figure 7D).

D2+D3 Receptor Dysregulation in *Hdc* KO and Heterozygous Mice

We examined D2+D3 receptor density in $Hdc^{+/-}$ and $Hdc^{-/-}$ mice using ^{3}H-raclopride binding to brain slices ex vivo, where there is no ambient DA. Raclopride binding was seen in SN (Figure 8A; Figure S6D) and striatum (Figure 8D; Figure S6E). In the SN, higher ^{3}H-raclopride binding was found in KOs and heterozygotes than in wild-type controls (Figures 8B and 8C). SN raclopride binding correlated with the number of KO alleles. This parallel to the human PET data establishes that this receptor change is causally attributable to *Hdc* genotype and strongly suggests that the abormality seen in vivo in patients reflects increased receptor density or affinity, rather than reduced [DA] in these structures.

Raclopride binding in the dorsal striatum showed a small but statistically significant reduction as a function of genotype (4%–14% reduction in +/− and −/− mice; Figures 8D and 8E). Regression analysis across genotypes and caudal-rostral location showed a significant inverse relationship between dorsal striatal raclopride binding and number of *Hdc* KO alleles (Figure 8E; Figure S6E), suggesting D2 downregulation in the dorsal striatum in *Hdc* KO mice. This reduction was not seen in the human PET data. This discrepancy may represent a species difference. Alternatively, our power to detect such a small difference may be limited due to the small number of subjects carrying the *Hdc* W317X mutation we were able to image.

This reduction in striatal D2+D3 binding and increased SN D2+D3 binding (Figures 7D, 8C, and 8E) may represent cellular responses to chronic elevation of striatal DA (Stanwood et al., 2000b). Consistent with this possibility, there was an inverse relationship between striatal (measured at caudal-rostral levels 5 and 6, where the genotype effect was most prominent; see Figures 8E and S6E) and nigral raclopride binding (Figure 8F).
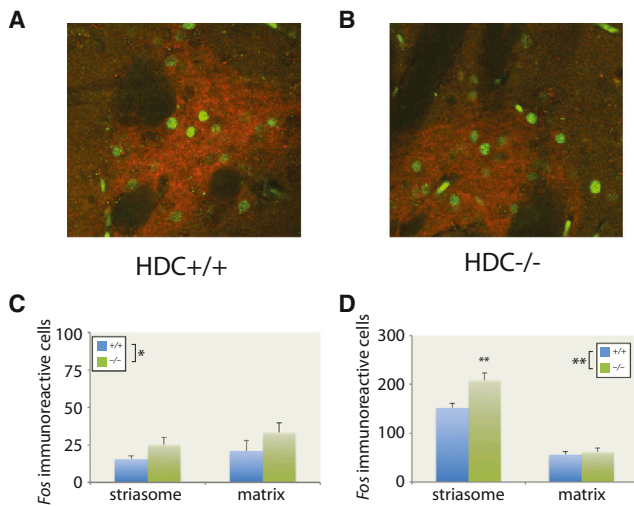
Figure 6. Elevated Striatal *Fos* Expression in *Hdc*$^{-/-}$ Mice Is Potentiated in Striasomes by Amphetamine

(A and B) *Fos*-positive cells (green) and μ-opioid immunoreactivity (red), a marker of striasomes (patches), 45 min after 5 mg/kg D-amphetamine in a *Hdc*$^{+/+}$ mouse (A) and a *Hdc*$^{-/-}$ mouse (B).

(C) At baseline, there was modestly but signifcantly increased *Fos* in *Hdc*$^{-/-}$ mice. RM-ANOVA, main effect of genotype, F[1,10] = 49.8, p < 0.001; effect of compartment and interaction, not significant; n = 6 slices from each of 6 mice per genotype. Post hoc genotype effects: *p < 0.05.

(D) After D-amphetamine, there was increased *Fos* expression in both compartments (note the y axis scale) but much more prominently in striasomes; striasomal activation was specifically potentiated in *Hdc*$^{-/-}$ mice. RM-ANOVA: main effect of genotype, F[1,10] = 8.7, p = 0.015; main effect of compartment, F[1,10] = 207, p < 0.0001; interaction, F[1,10] = 6.29, p = 0.03; n = 2 slices from each of 6 animals. Post hoc genotype effects: **p < 0.01. Group data are represented as mean ± SEM.

DISCUSSION

TS is a developmental neuropsychiatric disorder that is associated with basal ganglia abnormalities (Williams et al., 2013). Recent genetic findings have suggested, for the first time, that dysregulation of histaminergic neurotransmission represents a rare cause of TS (Bloch et al., 2011; Ercan-Sencicek et al., 2010; Fernandez et al., 2012; Karagiannidis et al., 2013). We have used parallel analysis in *Hdc* KO mice and in nine unique patients known to carry the hypomorphic *Hdc* W317X allele to confirm this association.

Hdc Disruption Causes Core Behavioral and Neurochemical Features of TS

The genetic relationship between the *Hdc* W317X mutation and TS in the index family is statistically compelling (Ercan-Sencicek et al., 2010). Direct evidence for causality, however, is not achievable with human genetic studies alone.

We find parallel TS-associated behavioral and neurochemical abnormalities in patients carrying the *Hdc* W317X mutation and *Hdc* KO and heterozygous mice (Table 1). This provides strong evidence for the causal association between *Hdc* disruption and TS.

HA Regulates Dopaminergic Modulation of the Basal Ganglia Circuitry

It has been speculated that HA regulates DA in the basal ganglia in vivo (Haas et al., 2008; Schlicker et al., 1994). *Hdc* KO mice were reported to exhibit increased DA turnover (Dere et al., 2003); indirect pharmacological enhancement of central HA modulates DA-associated stereotypical behaviors (Joshi et al., 1981; Kitanaka et al., 2010; Paul et al., 2000). We find that exogenously administered HA profoundly reduces striatal DA levels (Figure 5A). In KO mice, we do not observe a clear change in baseline DA during the day but find a dysregulation that emerges during the animals' active phase, when HA levels in wild-type animals are highest (Figures 5B–5D).

The direct measure of DA (Figure 5) and the alterations in baseline *Fos* (Figure 6) suggest chronic, if mild and fluctuating, elevation of DA. The pattern of receptor alterations observed in the *Hdc* KO mice is consistent with the pattern expected after chronic dopaminergic hyperstimulation. This pattern is partially recapitulated in patients carrying the *Hdc* W317X mutation, in whom we find elevated binding by the D2+D3 agonist radiotracer ^{11}C-PHNO in the SN and, less profoundly, in the GP.

These data represent in vivo evidence in humans of a direct relationship between alterations in histaminergic neurotransmission and dopaminergic modulation of the basal ganglia circuitry.

Histaminergic Regulation of Information Processing in the Basal Ganglia

Despite the prominent expression of HA receptors in the basal ganglia, the functional effects of HA in this circuitry have not been extensively studied. Histaminergic axons in the striatum are relatively sparse and make few direct synaptic contacts, (Takagi et al., 1986); however, the axons are varicose (Takagi et al., 1986), and the wild-type striatum contains a high amount of HDC protein (Krusong et al., 2011). Several striatal synapses are regulated by HA in vitro (Ellender et al., 2011). The ability of HA to reduce striatal DA levels (Figure 5A) suggests that it may provide a brake on DA.

The circadian modulation of HA (Figure 5B) suggests that it may produce a circadian modulation of striatal information processing, although direct evidence for this speculation is lacking. This circadian modulation of HA may have important implications for pathophysiology. Tics in TS typically do not occur during sleep. If the emergence (or amplification) of an abnormality in DA that we observe in these mice (Figures 5C and 5D) is a general phenomenon, it may help explain this observation in TS and other movement disorders.

Dysregulation of dopaminergic modulation in the basal ganglia is unlikely to be the only relevant effect of reduced histaminergic tone. Hypothalamic HDC-expressing neurons project widely throughout the CNS. Indeed, other investigations in the *Hdc* KO mice indicate abnormalities in hippocampal and cortical function (e.g., Acevedo et al., 2006; Dere et al., 2004). The inhibitory H3 receptor is expressed presynaptically on dopaminergic terminals and may explain the ability of HA to reduce striatal DA, but it is also expressed presynaptically on other cell types and regulates other neurotransmitters (Ellender et al., 2011; Haas et al., 2008; Schlicker et al., 1994). HA H1 and H2 receptors are also expressed prominently in the basal ganglia circuitry
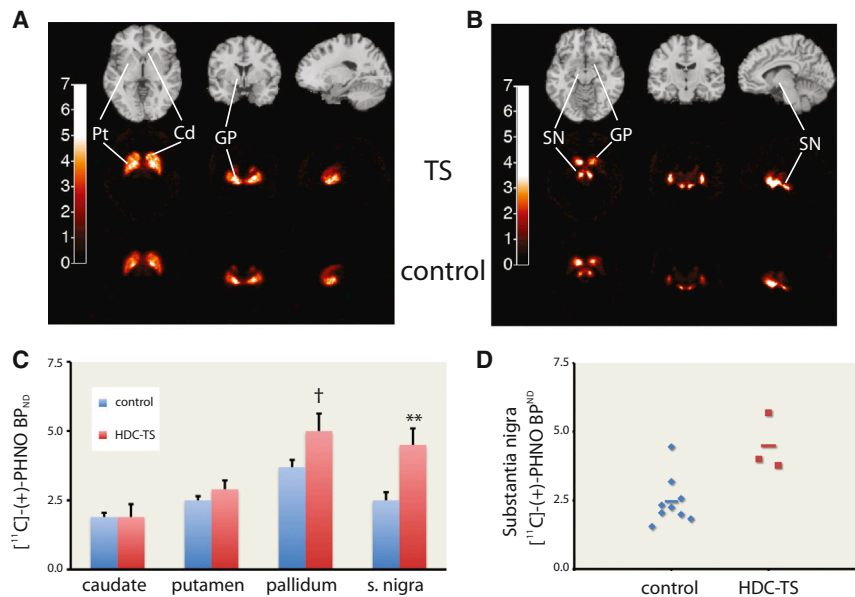
Figure 7. Elevated SN D2/D3 Binding in *Hdc* W317X Patients

(A) [^{11}C]-PHNO binding potential in the striatum and GP. Top row, structural MRI images for anatomical reference; middle row, PHNO binding in TS patients carrying the *Hdc* W317X allele; bottom row, PHNO binding in matched control subjects.

(B) [^{11}C]-PHNO binding in more inferior, posterior, and medial sections, showing the GP and SN.

(C) Patients carrying the *Hdc* W317X allele showed normal [^{11}C]-PHNO binding in caudate and putamen but elevated binding in GP and SN. RM-ANOVA: main effect of group: $F[1,10] = 7.54$; $p = 0.035$; main effect of region: $F[3,30] = 33.48$, $p < 0.001$; Group × Region interaction, $F[3,30] = 6.85$, $p = 0.001$. $n = 3$ *Hdc* W317X patients, 9 controls (mean ± SEM). BP$_{ND}$, [^{11}C]-PHNO binding potential. †Uncorrected $p < 0.05$; **uncorrected $p < 0.01$, significant after Bonferroni correction. Group data are represented as mean ± SEM.

(D) Separation between patients and controls was particularly striking in SN (individual data points and group means are shown). Mann-Whitney U test: $p = 0.03$. BP$_{ND}$, [^{11}C]-PHNO binding potential. See also Table S2, Table S3, and Figure S6.

and throughout the brain (Haas et al., 2008; Traiffort et al., 1994; Traiffort et al., 1995; Zhou et al., 2006). How alterations in information processing beyond the basal ganglia contribute to pathophysiological changes relevant to TS is an important area for future study.

Hdc KO Mice as a Pathophysiologically Realistic Model of TS

Hdc abnormalities are unlikely to explain more than a small fraction of TS cases. However, modeling this rare cause of TS in an animal is likely to lead to generalizable pathophysiological insights.

Animal models have traditionally been evaluated on the basis of face validity (their recapitulation of recognizable signs and symptoms of the modeled disease), predictive validity (their ability to predict what drugs will be efficacious in disease), and construct validity (their recapitulation of hypothesized core pathophysiology). The first two are problematic in the case of neuropsychiatric disease (Nestler and Hyman, 2010; Pittenger, 2011). Face validity raises challenges because of the subtle and subjective nature of psychiatric symptomatology. Not all repetitive behaviors are tics. Clinically, tics are characterized by premonitory urges, the fact that they can often be resisted at least to a limited extent, and the way in which that tic emission discharges a sense of discomfort. None of these can be readily evaluated in a mouse model. Predictive validity also must contend with a lack of specificity. D2 antagonists, for example, are used in the treatment of TS, but also for psychosis, bipolar disorder, depression, OCD, delirium, and other conditions. They are not efficacious in every case. In this context, response to a medication does not uniquely validate an animal model, and a lack of response does not invalidate it. Construct validity is critical to the elaboration of a pathophysiologically informative model.

The *Hdc* KO mice derive construct validity from a high-penetrance disease-associated allele. Behavioral phenotypes endow the model with reinforcing face validity (Figures 1, 2, 3, and 4). Enhanced stereotypy and reduced PPI are not specific to TS, but in the context of the inherent construct validity of the *Hdc* KO mouse, they confirm that relevant processes have been disrupted. Similarly, the mitigation of tic-like stereotypies by haloperidol (Figure 2) is not a TS-specific result, but this predictive validity further reinforces the *Hdc* KO mouse as a faithful recapitulation of core aspects of the pathophysiology of disease.

Patients carrying the *Hdc* W317X are not likely to be wholly deficient in brain HA; their wild-type allele should permit some production. Therefore, it may be that *Hdc*$^{+/-}$ mice more faithfully recapitulate the disease state than full KOs. Given this, it is important that *Hdc*$^{+/-}$ mice show a phenotype intermediate between wild-type and full KO mice in all key experiments: the potentiation of tic-like stereotypy (Figures 1D, 1E, 2B, and 2D), the impairment in PPI (Figure 4B), and the dysregulation of D2+D3 receptors in the basal ganglia (Figures 8C and 8E).

Clinical Implications

Excessive movements can be produced by increased activity of the striatonigral (direct) pathway or reduced activity of the striatopallidal (indirect) pathway. Tics may derive from hypoactivity of the indirect pathway, leading to deficient inhibition of off-target movements (Albin, 2006; Mink, 2001; Williams et al., 2013). Chronic moderate increases in DA in *Hdc* KO animals might produce such a state. The D2 receptor expressed by MSNs of the indirect pathway has a higher affinity for DA than D1 receptor (Rankin et al., 2010) and may be more responsive to modest, chronic elevations in DA. Tonically increased D2 tone would lead to tonically reduced activity in MSNs of the
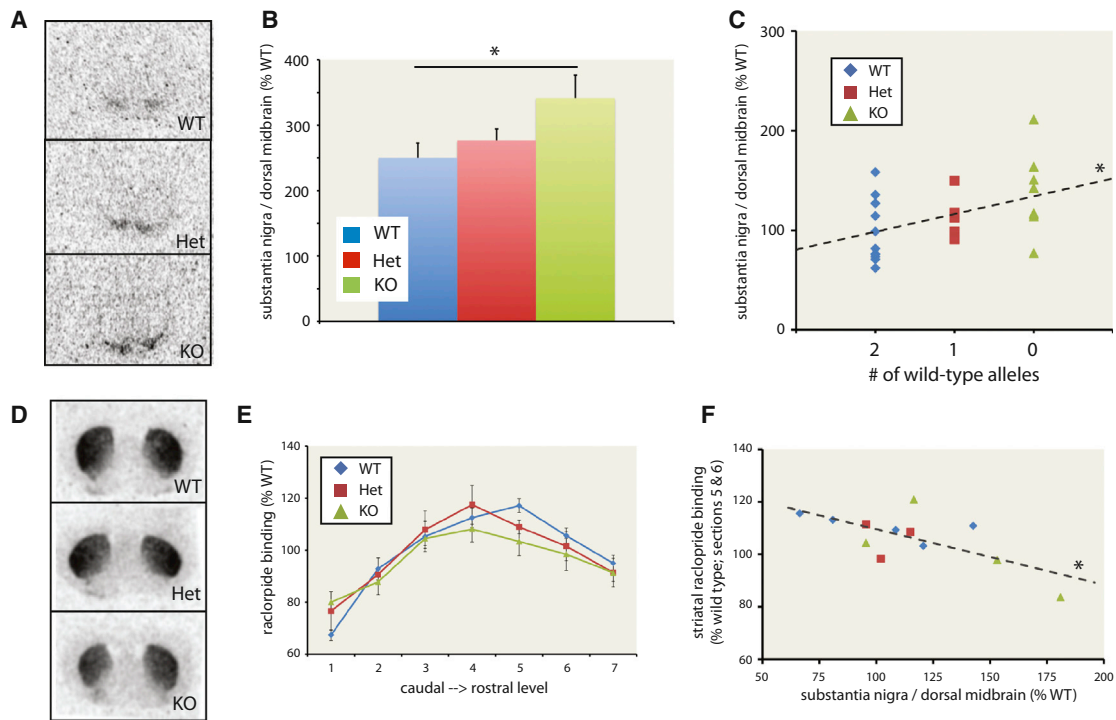
Figure 8. Altered D2/D3 Binding in *Hdc*-KO Mice

(A) Ex vivo raclopride binding in SN of $Hdc^{+/+}$, $Hdc^{+/-}$, and $Hdc^{-/-}$ mice.

(B) Normalized SN binding was elevated in $Hdc^{+/-}$ and $Hdc^{-/-}$ mice relative to +/+ controls. *p < 0.05.

(C) Binding correlated with the number of KO alleles (r = 0.445; β = 31.795; p = 0.02). *p < 0.05.

(D) Stronger raclopride binding was seen in striatum, reflecting the high density of D2 receptors there.

(E) Regression analysis across genotypes and caudal-rostral location showed a small but significant inverse relationship between dorsal striatal raclopride binding and number of HDC KO alleles, suggesting D2 downregulation in the dorsal striatum in HDC KO mice (β = −3.613, p = 0.017 for alleles; β = 6.01, p < 0.001 for rostral-caudal level).

(F) Raclopride binding in the midstriatum (A-P levels 5–6), where the effect of genotype on binding was most pronounced, was negatively correlated with nigral raclopride binding in the same animals: r = −0.682; p = 0.015. All data represented as individual data points or as mean ± SEM. *p < 0.05. n = 5 $Hdc^{+/+}$ (12 SN slices, 23 striatal slices), 4 $Hdc \pm$ (8 SN slices, 15 striatal slices), 6 $Hdc^{-/-}$ (8 SN slices from 4 mice; 21 striatal slices).

Group data are represented as mean ± SEM. See also Figure S6.

indirect pathway (Mink, 2001); this would be mitigated by D2 blockade, as in Figure 2.

We find that HA repletion mitigates potentiated stereotypies in these animals (Figure 3). A similar effect was suggested by indirect pharmacological modulation of HA levels in wild-type mice (Joshi et al., 1981; Kitanaka et al., 2007; Paul et al., 2000). This suggests that increasing brain HA may be of therapeutic value in TS. Dietary supplementation with histidine might increase HA production (Kitanaka et al., 2010). H3 receptor antagonists may increase HA release by blocking inhibitory autoreceptors on histaminergic terminals (Flik et al., 2011), although their effect on other cells is a complication (Ellender et al., 2011; Schlicker et al., 1994). The generation of such testable hypotheses illustrates the potential utility of this pathophysiologically valid animal model.

EXPERIMENTAL PROCEDURES

More detailed methods are given in the Supplemental Experimental Procedures.

Mice

All mouse experiments were approved by the Yale University Institutional Animal Care and Use Committee (Assurance Number: A3230-01). Generation of *Hdc* KO mice has been described elsewhere (Ohtsu et al., 2001). Adult male mice, aged 3–9 months, were used in all experiments.

HDC Activity Assay and HA Quantification

The W317X mutation was introduced into the mouse *Hdc* gene using standard molecular cloning techniques. HDC enzymatic activity (Figure 1A) was quantified as previously described (Ercan-Sencicek et al., 2010). Quantification of tissue [HA] (Figure 1B) was performed as described previously (Krusong et al., 2011). Quantification of microdialysate [HA] (Figure 5B), which is two orders of magnitude lower, was by mass spectrometry.

Open Field Exploration and Stereotypy in Mice

Adult male mice were placed in an unfamiliar novel open-topped white opaque plexiglass box, and their exploratory activity was monitored for 20 min using both observation and a video tracking system (AnyMaze). After 20 min, D-amphetamine (Sigma; 8.5 mg/kg or 10 mg/kg) or saline was administered i.p., and monitoring was continued for another 30 min. A broad range of stereotypical behaviors were noted (Kelley, 2001); the vast majority of observed stereotypies consisted of repetitive focused sniffing movements, which are

Table 1. Summary of Parallel Findings in TS Patients Carrying the *Hdc* W317X Mutation and in *Hdc*⁻/⁻ and *Hdc*⁺/⁻ Mice

Characteristic	Patients with *Hdc* W317X Mutation	*Hdc*⁺/⁻ and *Hdc*⁻/⁻ Mice	Figure, Table, or Reference
HA biosynthesis	Reduced (in vitro)	Reduced in tissue and striatal microdialysate	Figures 1A, 1B, and 5B; Ohtsu et al., 2001
Tics/stereotypy	Motor, phonic tics	Potentiated stereotypy after threshold-dose amphetamine	Figures 1E, 1F, 2B, 3A, and 3B; Table 1
PPI	Reduced	Reduced	Figure 4
Striatal DA	Not directly measured	Increased in active-phase microdialysate	Figures 5C and 5D
Striatal DA signaling	Not directly measured	Increased striatal *Fos* expression at baseline and after amphetamine	Figure 6
SN D2/D3 binding	Increased by in vivo PHNO PET imaging	Increased by in vitro raclopride binding	Figure 7
Dorsal striatal D2/D3 binding	No evident change, by in vivo PHNO PET imaging	Modest decrease, by in vitro raclopride binding	Figure 8

The table is a summary of abnormalities found in TS patients carrying the *Hdc* W317X mutation and in *Hdc* haploinsufficient and/or KO mice.

reported (Movies S1, S2, and S3). For haloperidol pretreatment (Figure 2), animals were monitored in the environment for 20 min, then injected i.p. with haloperidol (Sigma, 0.3 or 0.6 mg/kg) and observed for a further 15 min, and then injected with amphetamine or saline as described earlier (Figure 2A). All animals in this experiment (Figure 2) received both haloperidol and saline, in counterbalanced order, 5–7 days apart; treatment order was included as an independent factor of no interest in the ANOVA.

Elevated Plus Maze in Mice
Elevated plus maze analysis was performed as described elsewhere (Lee et al., 2008).

HA Mitigation of Stereotypy
Pilot experiments showed surgical cannulation to reduce and delay amphetamine-induced stereotypies; to increase sensitivity, we extended our observation period and observed animals in higher ambient light in a clear-sided enclosure (a standard rat housing cage) rather than a larger opaque-sided open-field box. Cannulae were implanted i.c.v. using standard stereotaxic surgical technique; animals were allowed to recover for at least 5 days following surgery before behavioral testing. Locomotor activity was measured before and after administration by infrared beam-breaks on an open-field apparatus (Med Associates). Mice were habituated to the environment for 60 min before the first amphetamine treatment (Figure S3A). They were then briefly immobilized and treated i.c.v. with HA (20 μg in 1 μl sterile saline) (Kalivas, 1982; Kamei et al., 1983, 1984; Onodera and Ogura, 1981) or saline and then immediately injected i.p. with amphetamine (8.5 mg/kg). Stereotypical behaviors were measured at intervals over 90 min by a trained observer blind to animal genotype and drug treatment. The procedure was repeated 5–7 days later with the other treatment (saline or HA), in counterbalanced order.

Because of the longer observation period, quantification of stereotypy was performed by instantaneous sampling rather than continuous monitoring, using a well-validated method (Fray et al., 1980); the dependent measure is the total number of sampled 10 s intervals during which a behavior was present.

Startle and PPI of Startle
Startle to a broadband acoustic stimulus was measured using standard procedures as described elsewhere (Baldan Ramsey et al., 2011). The initial PPI experiment (Figures 4C and S4H–S4N) was performed using a 100 ms prepulse-pulse interval; replication in the dark phase (Figures 4F, S4O, and S4P) was performed using a 200 ms interval, which was found in pilot experiments (data not shown) to produce a more robust separation of genotypes.

In Vivo Microdialysis
Adult male mice were implanted unilaterally with a guide cannula targeted to the dorsal striatum using standard stereotaxic technique; animals for HA infu-

sion (Figure 5A) were simultaneously implanted contralaterally, with a cannula guide targeted for i.c.v. infusion. After habituation, microdialysate was collected in 30 min samples, and DA levels were measured using standard techniques (Tellez et al., 2013). Following microdialyisis, mice were euthanized and their brains were examined to establish cannula placement. Animals in which chromatograms suggested excessive bleeding or anatomical analysis indicated cannula misplacement were excluded, prior to data analysis.

HA Infusion with Microdialysis
After recovery from surgery, a microdialyisis cannula was inserted. Microdialysate was perfused at 2 μl/min and collected in 10 min aliquots. Following a 3 hr baseline, mice were briefly immobilized and HA (20 μg in 1 μl sterile saline) or an equivalent amount of saline was infused over 2 min; mice were then monitored for 90 more min. DA was measured subsequently using high-pressure liquid chromatography, as described earlier. All mice received both HA and saline, separated by 1 week, in counterbalanced order.

Fos Immunoreactivity
At 45 min following saline or D-amphetamine (5 mg/kg i.p. in sterile saline) administration, brains were removed, fixed overnight in 4% paraformaldehyde, and stored in 30% sucrose. Floating sections (30 μm) were immunostained following standard procedures (see Supplemental Experimental Procedures for details) with goat anti-c-*fos* (1:500, Santa Cruz Biotechnology) and rabbit anti-μ-opioid receptor (1:1,000, Immunostar) antibodies followed by Alexa Fluor-coupled secondary antibodies (Jackson Immnoresearch). Fluorescence was visualized on a confocal microscope. *Fos*-positive cells were counted in μ-positive (striasome) and μ-negative (matrix) compartments bilaterally in multiple slices per animal (Young et al., 1991).

Raclopride Binding in Mice
³H-raclopride binding to unfixed fresh frozen slices of mouse brain was determined as described previously (Fasano et al., 2009). Signal was visualized using a phosphor imager system (Cyclone Plus, Perkin Elmer). Images were analyzed using Photoshop (Adobe), as further described in the Supplemental Experimental Procedures and in Figure S6.

Human Subjects
All human testing was overseen by the Yale University Human Investigations Committee (Federalwide Assurance #00002571). Nine individuals from a single family who have previously been identified as having a current or past diagnosis of a tic disorder and as carrying the *Hdc* W317X mutation (Ercan-Sencicek et al., 2010) were evaluated for this study. Controls, matched for age and sex and (for PET imaging) for body mass index were recruited from the community through advertising. Patients and controls were assessed

using standard clinical instruments to confirm diagnoses and quantify symptomatology.

PPI in Patients
Auditory startle and PPI were assessed as previously described (Lipschitz et al., 2005) using the SR-HLAB system (San Diego Instruments).

PET Imaging
[^{11}C]-(+)-PHNO was prepared, and PET imaging was performed as described previously (Narendran et al., 2006; Tziortzi et al., 2011) (Table S3). Dynamic scan data were constructed with all corrections using the MOLAR algorithm (Carson et al., 2003). Arterial blood samples were collected throughout scanning to measure the arterial input function. [^{11}C]-(+)-PHNO volumes of distribution were quantified using the multilinear analysis MA1 (Ichise et al., 2002) using arterial input function data.

Statistical Analysis
All analysis was performed using PASW Statistics 18.0 (SPSS/IBM) in consultation with a biostatistician. The t tests, correlations, and ANOVA, with RM and/or covariance as appropriate, were used as described in the text and figure legends for each data set. Two-tailed tests with an α of 0.05 were used except where clear, directional a priori hypotheses justified an α of 0.1, as indicated.

In the analysis of focused-sniffing stereotypy following HA injected i.c.v. (Figure 3), parametric statistics were not appropriate because of the very low variance in the HA-treated groups (no stereotypy was seen at most time points), and nonparametric ANOVA-like statistics were used. The key PET finding of increased PHNO binding in the SN was confirmed using the nonparametric Mann-Whitney U test (Figure 5D) because of the low n in the TS group.

SUPPLEMENTAL INFORMATION

Supplemental Information includes Supplemental Experimental Procedures, six figures, three tables, and three movies and can be found with this article online at http://dx.doi.org/10.1016/j.neuron.2013.10.052.

REFERENCES

Acevedo, S.F., Ohtsu, H., Benice, T.S., Rizk-Jackson, A., and Raber, J. (2006). Age-dependent measures of anxiety and cognition in male histidine decarboxylase knockout (Hdc-/-) mice. Brain Res. *1071*, 113–123.

Ahmari, S.E., Risbrough, V.B., Geyer, M.A., and Simpson, H.B. (2012). Impaired sensorimotor gating in unmedicated adults with obsessive-compulsive disorder. Neuropsychopharmacology *37*, 1216–1223.

Albin, R.L. (2006). Neurobiology of basal ganglia and Tourette syndrome: striatal and dopamine function. Adv. Neurol. *99*, 99–106.

Albin, R.L., Young, A.B., and Penney, J.B. (1989). The functional anatomy of basal ganglia disorders. Trends Neurosci. *12*, 366–375.

Alexander, G.E., DeLong, M.R., and Strick, P.L. (1986). Parallel organization of functionally segregated circuits linking basal ganglia and cortex. Annu. Rev. Neurosci. *9*, 357–381.

Baldan Ramsey, L.C., Xu, M., Wood, N., and Pittenger, C. (2011). Lesions of the dorsomedial striatum disrupt prepulse inhibition. Neuroscience *180*, 222–228.

Bloch, M.H. (2008). Emerging treatments for Tourette's disorder. Curr. Psychiatry Rep. *10*, 323–330.

Bloch, M., State, M., and Pittenger, C. (2011). Recent advances in Tourette syndrome. Curr. Opin. Neurol. *24*, 119–125.

Braff, D., Stone, C., Callaway, E., Geyer, M., Glick, I., and Bali, L. (1978). Prestimulus effects on human startle reflex in normals and schizophrenics. Psychophysiology *15*, 339–343.

Canales, J.J., and Graybiel, A.M. (2000). A measure of striatal function predicts motor stereotypy. Nat. Neurosci. *3*, 377–383.

Carson, R.E., Barker, W., Liow, J.-S., and Johnson, C. (2003). Design of a motion-compensation OSEM list-mode algorithm for resolution-recovery reconstruction for the HRRT. Nuclear Science Symposium Conference Record, 2003 IEEE *5*, 3281–3285.

Castellanos, F.X., Fine, E.J., Kaysen, D., Marsh, W.L., Rapoport, J.L., and Hallett, M. (1996). Sensorimotor gating in boys with Tourette's syndrome and ADHD: preliminary results. Biol. Psychiatry *39*, 33–41.

Choi, E.Y., Yeo, B.T., and Buckner, R.L. (2012). The organization of the human striatum estimated by intrinsic functional connectivity. J. Neurophysiol. *108*, 2242–2263.

Crittenden, J.R., and Graybiel, A.M. (2011). Basal Ganglia disorders associated with imbalances in the striatal striosome and matrix compartments. Frontiers in neuroanatomy *5*, 59.

Davis, L.K., Yu, D., Keenan, C.L., Gamazon, E.R., Konkashbaev, A.I., Derks, E.M., Neale, B.M., Yang, J., Lee, S.H., Evans, P., et al. (2013). Partitioning the heritability of tourette syndrome and obsessive compulsive disorder reveals differences in genetic architecture. PLoS Genet. *9*, e1003864.

de Leeuw, A.S., Oranje, B., van Megen, H.J., Kemner, C., and Westenberg, H.G. (2010). Sensory gating and sensorimotor gating in medication-free obsessive-compulsive disorder patients. Int. Clin. Psychopharmacol. *25*, 232–240.

Dere, E., De Souza-Silva, M.A., Topic, B., Spieler, R.E., Haas, H.L., and Huston, J.P. (2003). Histidine-decarboxylase knockout mice show deficient nonreinforced episodic object memory, improved negatively reinforced water-maze performance, and increased neo- and ventro-striatal dopamine turnover. Learn. Mem. *10*, 510–519.

Dere, E., De Souza-Silva, M.A., Spieler, R.E., Lin, J.S., Ohtsu, H., Haas, H.L., and Huston, J.P. (2004). Changes in motoric, exploratory and emotional behaviours and neuronal acetylcholine content and 5-HT turnover in histidine decarboxylase-KO mice. Eur. J. Neurosci. *20*, 1051–1058.

Du, J.C., Chiu, T.F., Lee, K.M., Wu, H.L., Yang, Y.C., Hsu, S.Y., Sun, C.S., Hwang, B., and Leckman, J.F. (2010). Tourette syndrome in children: an updated review. Pediatr. Neonatol. *51*, 255–264.

Ellender, T.J., Huerta-Ocampo, I., Deisseroth, K., Capogna, M., and Bolam, J.P. (2011). Differential modulation of excitatory and inhibitory striatal synaptic transmission by histamine. J. Neurosci. *31*, 15340–15351.

Ercan-Sencicek, A.G., Stillman, A.A., Ghosh, A.K., Bilguvar, K., O'Roak, B.J., Mason, C.E., Abbott, T., Gupta, A., King, R.A., Pauls, D.L., et al. (2010). L-histidine decarboxylase and Tourette's syndrome. N. Engl. J. Med. *362*, 1901–1908.

Fasano, S., Pittenger, C., and Brambilla, R. (2009). Inhibition of CREB activity in the dorsal portion of the striatum potentiates behavioral responses to drugs of abuse. Front. Behav. Neurosci 3, 29, http://dx.doi.org/10.3389/neuro.08.029.2009.

Fauchey, V., Jaber, M., Caron, M.G., Bloch, B., and Le Moine, C. (2000). Differential regulation of the dopamine D1, D2 and D3 receptor gene expression and changes in the phenotype of the striatal neurons in mice lacking the dopamine transporter. Eur. J. Neurosci. 12, 19–26.

Fernandez, T.V., Sanders, S.J., Yurkiewicz, I.R., Ercan-Sencicek, A.G., Kim, Y.S., Fishman, D.O., Raubeson, M.J., Song, Y., Yasuno, K., Ho, W.S., et al. (2012). Rare copy number variants in tourette syndrome disrupt genes in histaminergic pathways and overlap with autism. Biol. Psychiatry 71, 392–402.

First, M.B., Spitzer, R.L., Gibbon, M., and Williams, J.B. (1997). Structured Clinical Interview for DSM-IV Axis I Disorders: Clinical Version (SCID-CV). (Washington, DC: American Psychiatric Press).

Flik, G., Dremencov, E., Cremers, T.I., Folgering, J.H., and Westerink, B.H. (2011). The role of cortical and hypothalamic histamine-3 receptors in the modulation of central histamine neurotransmission: an in vivo electrophysiology and microdialysis study. Eur. J. Neurosci. 34, 1747–1755.

Fray, P.J., Sahakian, B.J., Robbins, T.W., Koob, G.F., and Iversen, S.D. (1980). An observational method for quantifying the behavioural effects of dopamine agonists: contrasting effects of d-amphetamine and apomorphine. Psychopharmacology (Berl.) 69, 253–259.

Graff-Guerrero, A., Willeit, M., Ginovart, N., Mamo, D., Mizrahi, R., Rusjan, P., Vitcu, I., Seeman, P., Wilson, A.A., and Kapur, S. (2008). Brain region binding of the D2/3 agonist [11C]-(+)-PHNO and the D2/3 antagonist [11C]raclopride in healthy humans. Hum. Brain Mapp. 29, 400–410.

Graybiel, A.M. (2008). Habits, rituals, and the evaluative brain. Annu. Rev. Neurosci. 31, 359–387.

Grillner, S., Robertson, B., and Stephenson-Jones, M. (2013). The evolutionary origin of the vertebrate basal ganglia and its role in action selection. J. Physiol. 591, 5425–5431.

Haas, H.L., Sergeeva, O.A., and Selbach, O. (2008). Histamine in the nervous system. Physiol. Rev. 88, 1183–1241.

Haber, S.N., and Knutson, B. (2010). The reward circuit: linking primate anatomy and human imaging. Neuropsychopharmacology 35, 4–26.

Hoenig, K., Hochrein, A., Quednow, B.B., Maier, W., and Wagner, M. (2005). Impaired prepulse inhibition of acoustic startle in obsessive-compulsive disorder. Biol. Psychiatry 57, 1153–1158.

Ichise, M., Toyama, H., Innis, R.B., and Carson, R.E. (2002). Strategies to improve neuroreceptor parameter estimation by linear regression analysis. J. Cereb. Blood Flow Metab. 22, 1271–1281.

Jankovic, J., and Kurlan, R. (2011). Tourette syndrome: evolving concepts. Mov. Disord. 26, 1149–1156.

Joshi, V.V., Balsara, J.J., Jadhav, J.H., and Chandorkar, A.G. (1981). Effect of L-histidine and chlorcyclizine on apomorphine-induced climbing behaviour and methamphetamine stereotypy in mice. Eur. J. Pharmacol. 69, 499–502.

Kalivas, P.W. (1982). Histamine-induced arousal in the conscious and pentobarbital-pretreated rat. J. Pharmacol. Exp. Ther. 222, 37–42.

Kamei, C., Dabasaki, T., and Tasaka, K. (1983). Cataleptic effect of histamine induced by intraventricular injection in mice. Jpn. J. Pharmacol. 33, 1081–1084.

Kamei, C., Dabasaki, T., and Tasaka, K. (1984). Effect of intraventricular injection of histamine on the pinna reflex in mice. Jpn. J. Pharmacol. 35, 193–195.

Karagiannidis, I., Dehning, S., Sandor, P., Tarnok, Z., Rizzo, R., Wolanczyk, T., Madruga-Garrido, M., Hebebrand, J., Nöthen, M.M., Lehmkuhl, G., et al. (2013). Support of the histaminergic hypothesis in Tourette Syndrome: association of the histamine decarboxylase gene in a large sample of families. J. Med. Genet. 50, 760–764.

Kelley, A.E. (2001). Measurement of rodent stereotyped behavior. Curr. Protoc. Neurosci. 8, 8.8, http://dx.doi.org/10.1002/0471142301.ns0808s04.

Kitanaka, J., Kitanaka, N., Tatsuta, T., Morita, Y., and Takemura, M. (2007). Blockade of brain histamine metabolism alters methamphetamine-induced expression pattern of stereotypy in mice via histamine H1 receptors. Neuroscience 147, 765–777.

Kitanaka, J., Kitanaka, N., Tatsuta, T., Miyoshi, A., Koumoto, A., Tanaka, K., Nishiyama, N., Morita, Y., and Takemura, M. (2010). Pretreatment with l-histidine produces a shift from methamphetamine-induced stereotypical biting to persistent locomotion in mice. Pharmacol. Biochem. Behav. 94, 464–470.

Kohl, S., Heekeren, K., Klosterkötter, J., and Kuhn, J. (2013). Prepulse inhibition in psychiatric disorders—apart from schizophrenia. J. Psychiatr. Res. 47, 445–452.

Krusong, K., Ercan-Sencicek, A.G., Xu, M., Ohtsu, H., Anderson, G.M., State, M.W., and Pittenger, C. (2011). High levels of histidine decarboxylase in the striatum of mice and rats. Neurosci. Lett. 495, 110–114.

Kurlan, R. (2010). Clinical practice. Tourette's Syndrome. N. Engl. J. Med. 363, 2332–2338.

Kwak, C.H., and Jankovic, J. (2002). Tourettism and dystonia after subcortical stroke. Movement disorders: official journal of the Movement Disorder Society 17, 821–825.

Leckman, J.F., Riddle, M.A., Hardin, M.T., Ort, S.I., Swartz, K.L., Stevenson, J., and Cohen, D.J. (1989). The Yale Global Tic Severity Scale: initial testing of a clinician-rated scale of tic severity. J. Am. Acad. Child Adolesc. Psychiatry 28, 566–573.

Leckman, J.F., Bloch, M.H., Smith, M.E., Larabi, D., and Hampson, M. (2010). Neurobiological substrates of Tourette's disorder. J. Child Adolesc. Psychopharmacol. 20, 237–247.

Lee, A.S., Duman, R.S., and Pittenger, C. (2008). A double dissociation revealing bidirectional competition between striatum and hippocampus during learning. Proc. Natl. Acad. Sci. USA 105, 17163–17168.

Lipschitz, D.S., Mayes, L.M., Rasmusson, A.M., Anyan, W., Billingslea, E., Gueorguieva, R., and Southwick, S.M. (2005). Baseline and modulated acoustic startle responses in adolescent girls with posttraumatic stress disorder. J. Am. Acad. Child Adolesc. Psychiatry 44, 807–814.

McCairn, K.W., Bronfeld, M., Belelovsky, K., and Bar-Gad, I. (2009). The neurophysiological correlates of motor tics following focal striatal disinhibition. Brain 132, 2125–2138.

Mink, J.W. (2001). Neurobiology of basal ganglia circuits in Tourette syndrome: faulty inhibition of unwanted motor patterns? Adv. Neurol. 85, 113–122.

Narendran, R., Slifstein, M., Guillin, O., Hwang, Y., Hwang, D.R., Scher, E., Reeder, S., Rabiner, E., and Laruelle, M. (2006). Dopamine (D2/3) receptor agonist positron emission tomography radiotracer [11C]-(+)-PHNO is a D3 receptor preferring agonist in vivo. Synapse 60, 485–495.

Nestler, E.J., and Hyman, S.E. (2010). Animal models of neuropsychiatric disorders. Nat. Neurosci. 13, 1161–1169.

O'Rourke, J.A., Scharf, J.M., Yu, D., and Pauls, D.L. (2009). The genetics of Tourette syndrome: a review. J. Psychosom. Res. 67, 533–545.

Ohtsu, H., Tanaka, S., Terui, T., Hori, Y., Makabe-Kobayashi, Y., Pejler, G., Tchougounova, E., Hellman, L., Gertsenstein, M., Hirasawa, N., et al. (2001). Mice lacking histidine decarboxylase exhibit abnormal mast cells. FEBS Lett. 502, 53–56.

Onodera, K., and Ogura, Y. (1981). Advances in histamine research. In Advances in Histamine Research, B. Uvnäs and K. Tasaka, eds. (Oxford: Pergamon Press), pp. 127–136.

Paul, V.N., Chopra, K., and Kulkarni, S.K. (2000). Modulation of motor functions involving central dopaminergic system by L-histidine. Indian J. Exp. Biol. 38, 988–993.

Payer, D.E., Behzadi, A., Kish, S.J., Houle, S., Wilson, A.A., Rusjan, P.M., Tong, J., Selby, P., George, T.P., McCluskey, T., and Boileau, I. (2013). Heightened D3 Dopamine Receptor Levels in Cocaine Dependence and Contributions to the Addiction Behavioral Phenotype: A Positron Emission Tomography Study with [(11)C]-(+)-PHNO. Neuropsychopharmacology. Published online August 7, 2013. http://dx.doi.org/10.1038/npp.2013.192.

Pittenger, C. (2011). Pathophysiological modeling of obsessive-compulsive disorder: challenges, and progress. Biol. Psychiatry 70, 1002–1003.

Rabiner, E.A., Slifstein, M., Nobrega, J., Plisson, C., Huiban, M., Raymond, R., Diwan, M., Wilson, A.A., McCormick, P., Gentile, G., et al. (2009). In vivo quantification of regional dopamine-D3 receptor binding potential of (+)-PHNO: Studies in non-human primates and transgenic mice. Synapse 63, 782–793.

Rankin, M.L., Hazelood, L.A., Free, R.B., Namkung, Y., Rex, E.B., Roof, R.A., and Sibley, D.R. (2010). Molecular pharmacology of the dopamine receptors. In The Dopamine Handbook, L.L. Iversen, S.B. Dunnett, S.D. Iversen, and A. Bjorkund, eds. (New York: Oxford University Press), pp. 63–87.

Scharf, J.M., Yu, D., Mathews, C.A., Neale, B.M., Stewart, S.E., Fagerness, J.A., Evans, P., Gamazon, E., Edlund, C.K., Service, S.K., et al. (2013). Genome-wide association study of Tourette's syndrome. Mol. Psychiatry 18, 721–728. Published online August 14, 2012. http://dx.doi.org/10.1038/mp.2012.69.

Schlicker, E., Malinowska, B., Kathmann, M., and Göthert, M. (1994). Modulation of neurotransmitter release via histamine H3 heteroreceptors. Fundam. Clin. Pharmacol. 8, 128–137.

Shmelkov, S.V., Hormigo, A., Jing, D., Proenca, C.C., Bath, K.G., Milde, T., Shmelkov, E., Kushner, J.S., Baljevic, M., Dincheva, I., et al. (2010). Slitrk5 deficiency impairs corticostriatal circuitry and leads to obsessive-compulsive-like behaviors in mice. Nat. Med. 16, 598–602.

Singer, H.S., Szymanski, S., Giuliano, J., Yokoi, F., Dogan, A.S., Brasic, J.R., Zhou, Y., Grace, A.A., and Wong, D.F. (2002). Elevated intrasynaptic dopamine release in Tourette's syndrome measured by PET. Am. J. Psychiatry 159, 1329–1336.

Stanwood, G.D., Artymyshyn, R.P., Kung, M.P., Kung, H.F., Lucki, I., and McGonigle, P. (2000a). Quantitative autoradiographic mapping of rat brain dopamine D3 binding with [(125)I]7-OH-PIPAT: evidence for the presence of D3 receptors on dopaminergic and nondopaminergic cell bodies and terminals. J. Pharmacol. Exp. Ther. 295, 1223–1231.

Stanwood, G.D., Lucki, I., and McGonigle, P. (2000b). Differential regulation of dopamine D2 and D3 receptors by chronic drug treatments. J. Pharmacol. Exp. Ther. 295, 1232–1240.

State, M.W. (2011). The genetics of Tourette disorder. Curr. Opin. Genet. Dev. 21, 302–309.

Swerdlow, N.R. (2012). Update: Studies of prepulse inhibition of startle, with particular relevance to the pathophysiology or treatment of Tourette Syndrome. Neurosci. Biobehav. Rev.

Swerdlow, N.R., Karban, B., Ploum, Y., Sharp, R., Geyer, M.A., and Eastvold, A. (2001). Tactile prepuff inhibition of startle in children with Tourette's syndrome: in search of an "fMRI-friendly" startle paradigm. Biol. Psychiatry 50, 578–585.

Takagi, H., Morishima, Y., Matsuyama, T., Hayashi, H., Watanabe, T., and Wada, H. (1986). Histaminergic axons in the neostriatum and cerebral cortex of the rat: a correlated light and electron microscopic immunocytochemical study using histidine decarboxylase as a marker. Brain Res. 364, 114–123.

Tellez, L.A., Medina, S., Han, W., Ferreira, J.G., Licona-Limón, P., Ren, X., Lam, T.T., Schwartz, G.J., and de Araujo, I.E. (2013). A gut lipid messenger links excess dietary fat to dopamine deficiency. Science 341, 800–802.

Terrados, G., Finkernagel, F., Stielow, B., Sadic, D., Neubert, J., Herdt, O., Krause, M., Scharfe, M., Jarek, M., and Suske, G. (2012). Genome-wide localization and expression profiling establish Sp2 as a sequence-specific transcription factor regulating vitally important genes. Nucleic Acids Res. 40, 7844–7857.

Traifort, E., Leurs, R., Arrang, J.M., Tardivel-Lacombe, J., Diaz, J., Schwartz, J.C., and Ruat, M. (1994). Guinea pig histamine H1 receptor. I. Gene cloning, characterization, and tissue expression revealed by in situ hybridization. J. Neurochem. 62, 507–518.

Traifort, E., Vizuete, M.L., Tardivel-Lacombe, J., Souil, E., Schwartz, J.C., and Ruat, M. (1995). The guinea pig histamine H2 receptor: gene cloning, tissue expression and chromosomal localization of its human counterpart. Biochem. Biophys. Res. Commun. 211, 570–577.

Turetsky, B.I., Calkins, M.E., Light, G.A., Olincy, A., Radant, A.D., and Swerdlow, N.R. (2007). Neurophysiological endophenotypes of schizophrenia: the viability of selected candidate measures. Schizophr. Bull. 33, 69–94.

Tziortzi, A.C., Searle, G.E., Tzimopoulou, S., Salinas, C., Beaver, J.D., Jenkinson, M., Laruelle, M., Rabiner, E.A., and Gunn, R.N. (2011). Imaging dopamine receptors in humans with [11C]-(+)-PHNO: dissection of D3 signal and anatomy. Neuroimage 54, 264–277.

Volkow, N.D., Fowler, J.S., Wang, G.J., Baler, R., and Telang, F. (2009). Imaging dopamine's role in drug abuse and addiction. Neuropharmacology 56 (Suppl. 1), 3–8.

Welch, J.M., Lu, J., Rodriguiz, R.M., Trotta, N.C., Peca, J., Ding, J.D., Feliciano, C., Chen, M., Adams, J.P., Luo, J., et al. (2007). Cortico-striatal synaptic defects and OCD-like behaviours in Sapap3-mutant mice. Nature 448, 894–900.

White, F.J., and Wang, R.Y. (1984). A10 dopamine neurons: role of autoreceptors in determining firing rate and sensitivity to dopamine agonists. Life Sci. 34, 1161–1170.

Williams, K., Bloch, M.H., State, M., and Pittenger, C. (2013). Tourette syndrome and tic disorders. In Neurobiology of Mental Illness, Fourth Edition, D.S. Charney, E.J. Nestler, P. Sklar, and J.D. Buxbaum, eds. (New York: Oxford University Press), pp. 1048–1060.

Wong, D.F., Brasić, J.R., Singer, H.S., Schretlen, D.J., Kuwabara, H., Zhou, Y., Nandi, A., Maris, M.A., Alexander, M., Ye, W., et al. (2008). Mechanisms of dopaminergic and serotonergic neurotransmission in Tourette syndrome: clues from an in vivo neurochemistry study with PET. Neuropsychopharmacology 33, 1239–1251.

Young, S.T., Porrino, L.J., and Iadarola, M.J. (1991). Cocaine induces striatal c-fos-immunoreactive proteins via dopaminergic D1 receptors. Proc. Natl. Acad. Sci. USA 88, 1291–1295.

Zhou, F.W., Xu, J.J., Zhao, Y., LeDoux, M.S., and Zhou, F.M. (2006). Opposite functions of histamine H1 and H2 receptors and H3 receptor in substantia nigra pars reticulata. J. Neurophysiol. 96, 1581–1591.